Zhao Yanping, Gong Jianming*, Wang Xiaowei and Li Qingnan

Creep Behaviors Calculated by Varying Material Constants Obtained from Different Stress Regions for a Closed-End P91 Pipe

DOI 10.1515/htmp-2015-0002
Received January 4, 2015; accepted April 4, 2015

Abstract: In order to predict the creep life of a component at high temperature both accurately and economically, continuum damage mechanics approach is used based on experimental creep data. However, material constants used in the models have a great relationship with the performed stress range of creep tests. In this paper, several sets of material constants were obtained from a wide range of stresses on P91 steel. The creep damage tolerance parameter was used to classify these sets, and the modified continuum damage mechanics model was used to investigate a pipe under closed-end condition. Results have illustrated the main difference lies on the tertiary stage while slight difference on the primary and secondary stages, and the contribution of the tertiary stage to the total damage decreased when using material constants from higher stress region.

Keywords: material constants, creep damage tolerance parameter, modified continuum damage mechanics model

Introduction

P91 steels are widely used in the piping systems operating at elevated temperature for its excellent creep strength. One of its main concerns is to predict the lifetime of these pipes under creep condition, especially having been in service for more than 150,000 h.

Recently, continuum damage mechanics (CDM) cooperated with the finite element (FE) method has been shown to be useful in predicting the creep conditions of engineering components.

Despite the typical creep damage constitutive equations [1, 2], several modified forms of constitutive equations have been proposed. Leckie and Hayhurst [3] have considered the effect by introducing the triaxial stress state material constant α. Liu and Murakami et al. [4] have addressed the issue of high strain/damage rates when the damage parameter approaches unity. Dyson [5] used a sinh function employing three state variables to take into account the discrepancy between experimental and predicted results.

In their works, the material constants in the constitutive equations are very important to the accuracy of the models. Their values were derived from the creep curves of uniaxial and notched bar testing in the laboratory conditions, and the creep properties are generally dependent on material, temperature, strain rate and the stress level. The tested stress level will affect the creep damage mechanisms, correspondingly leading to different material constants. However, the stress range dependency is generally very weak if the stress range involved is not large. Therefore, stress range dependent creep properties may only need to be considered, when a significant stress range effect has been identified from experiment. Many works have been done to classify creep damage mechanisms under different stresses. Creep damage tolerance parameter defined as $\lambda = \varepsilon_f/(\dot{\varepsilon}_{min} \cdot t_f)$, where ε_f is strain to failure, $\dot{\varepsilon}_{min}$ is minimum creep strain rate and t_f rupture life is an important outcome of CDM approach indicating the damage to initiate tertiary creep. Ashby and Dyson [6] demonstrated that each damage micromechanism, when acting alone, results in a characteristic λ value. The variation of λ value is in close connection with the shape of creep curves at different stresses. Thus, it can provide a basis to CDM approach when considering damage mechanisms related to the tertiary stage.

In this work, a modified Kachanov–Rabotnov constitutive model which accounts for the effects of creep damage inhomogeneity [7] was used to simulate an internally pressurized pipe under closed-end condition. In this model, material is considered as a composite consisted of many types of microelements or phases with different damage behaviors based on micro-mechanics consideration, and these elements are then described by Kachanov–Rabotnov equations with material damage constants. In order to classify the creep damage mechanism, creep curves of P91 under a wide range of stresses is analyzed with decreasing λ value. In all, three material constant sets have been obtained from the low, middle and high stress regions.

***Corresponding author: Gong Jianming,** School of Mechanical and Power Engineering, Nanjing Tech University, Nanjing, Jiangsu, China, E-mail: gongjm@njtech.edu.cn
Zhao Yanping, Wang Xiaowei, Li Qingnan, School of Mechanical and Power Engineering, Nanjing Tech University, Nanjing, Jiangsu, China

Theoretical background

Recently, the continuum damage constitutive equations proposed by Kachanov [1] and Rabotnov [2] have been used to model the creep curve. These equations are as follows:

$$\frac{d\varepsilon^c}{dt} = \frac{B\sigma^n}{(1-D)^m} \tag{1}$$

$$\frac{dD}{dt} = \frac{A}{\phi+1}\frac{\sigma^\upsilon}{(1-D)^\phi} \tag{2}$$

where B, n, m, A, υ and Φ are material constants, which are obtained from the fitting curves of experimental strain versus time. D is the damage variable varying from 0 (no damage) to 1 (failure). Thus, the life of materials under creep condition can be calculated when the damage factor D approaches 1 at the failure point.

In order to obtain more accurate results, a modified Kachanov–Rabotnov constitutive model considering the inhomogeneity damage [7] is used in this work:

$$\frac{d\varepsilon^c_{ij}}{dt} = \frac{3}{2}B\sigma_e^{n-1}s_{ij}[(1-\rho)+\rho(1-D)^{-n}] \tag{3}$$

$$\frac{dD}{dt} = g\frac{A}{\phi+1}\frac{[\alpha\sigma_1+(1-\alpha)\sigma_e]^\upsilon}{(1-D)^\phi} \tag{4}$$

$$D_{\text{cr}} = 1-(1-g)^{\frac{1}{\phi+1}} \tag{5}$$

where σ_1 and σ_e are the maximum principal stress and equivalent (von Mises) stress, respectively. ε_{ij} is the creep strain tensor, S_{ij} is the deviatoric stress tensor and α is to describe the multi-axial stress state of materials. D and D_cr are the damage variable and critical damage, respectively. The creep life can be estimated when D/D_cr reaches the value 0.99. Despite B, n, m, A, υ and Φ, two additional constants ρ and g are required to define the material creep behavior. These two constants are related to the effect of inhomogeneity of the damage.

Integration of eq. (4) from $D=0$–1, and eq. (3) with t from 0 to t leads to an expression between creep strain versus time, i.e.

$$\varepsilon^c = \dot{\varepsilon}^c_{\text{min}}t_\text{f}\left[(1-\rho)(t/t_\text{f})+\frac{\rho}{g(1-\beta)}\left[1-\left(1-g\frac{t}{t_\text{f}}\right)^{1-\beta}\right]\right] \tag{6}$$

where

$$\dot{\varepsilon}^c_{\text{min}} = B\sigma_c^n \tag{7}$$

$$t_\text{f} = \frac{1}{A\sigma_c^\upsilon} \tag{8}$$

$$\beta = \frac{n}{\phi+1} \tag{9}$$

Normalized form of eq. (6) can be represented as follows:

$$\frac{\varepsilon}{\varepsilon_\text{f}} = \frac{(1-\rho)\frac{t}{t_\text{f}}}{\lambda} + \frac{\rho\left[1-\left(1-g\frac{t}{t_\text{f}}\right)^{(1-\beta)}\right]}{g(1-\beta)\lambda} \tag{10}$$

where λ is the damage tolerance factor and

$$\lambda = \frac{\varepsilon_\text{f}}{\dot{\varepsilon}^c_{\text{min}}\,t_\text{f}} \tag{11}$$

FE analysis

Closed-end straight pipe model

FE model was conducted to simulate a realistic main steam P91 pipe in UK power plant. The main dimensions of this pipe are OD = 355.6 mm and T = 63.5 mm (see Figure 1). The meshes used in this investigation are asymmetrical four-node elements (CAX4). Boundary

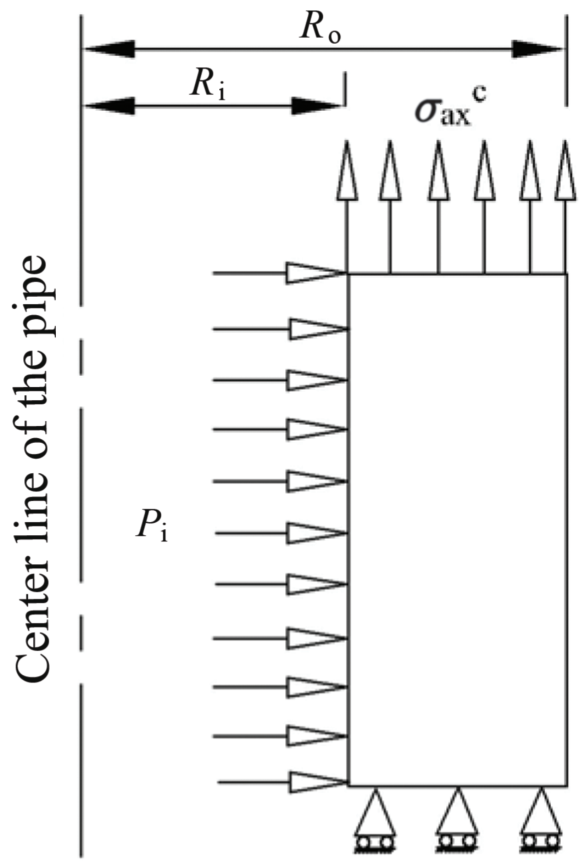

Figure 1: Diagram showing the principal dimensions (mm) and loading of the P91 pipe (R_o = 177.8 and R_i = 114.3).

conditions were applied to the pipe ends to prevent the translation of the model. In this paper, creep continuum damage analysis was conducted on the pipe with an internal pressure $p_i = 16.55$ MPa. In addition, an axial load which is equal to the mean axial stress $\sigma^c_{ax} = 11.66$ MPa was applied on both pipe ends, where σ^c_{ax} is the stress under closed-end condition [8] and calculated by

$$\sigma^c_{ax} = \frac{p_i}{(R_o/R_i)^2 - 1} \tag{12}$$

Material properties and data

Creep data of P91 steel shown in Figure 2 is used for simulations [9]. The material constants are obtained by analyzing the creep curves at 650°C at stress levels of 70, 82, 87, 93 and 100 MPa. Different sets of material constants were obtained from this range of stresses, which had a great influence on the creep damage and life time. The damage calculations were continued until the damage $D/D_{cr} = 0.99$ has extended to the entire pipe thickness in simulations.

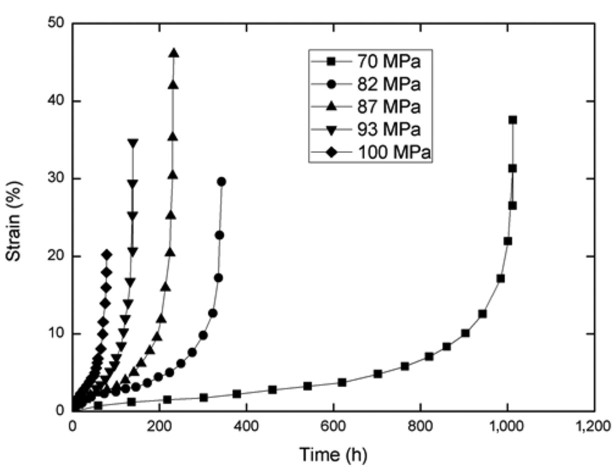

Figure 2: Uniaxial creep strain curves tested at 650°C for a wide range stresses [9].

B and n are calculated from the best fitting line between minimum creep strain rate and applied stress on log–log scale (eq. 7). The slope of this line is the value of n and its intercept is log(B). Similarity, best fitting line between failure time and applied stress on log-log scale is used to obtain A and υ (eq. 8). The slope of the line is the value of $-\upsilon$ and the intercept is $-\log(A)$. On the other hand, multi-axial material constant α was determined from the

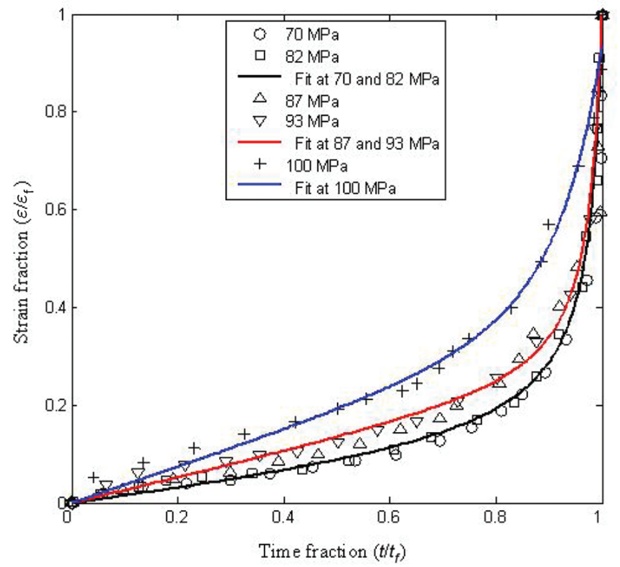

Figure 3: Strain fraction ($\varepsilon/\varepsilon_f$) as a function of time fraction (t/t_f) in a range of stress regions at 650°C for P91 steel. The plots are fitted according to eq. (10) and the symbols represent experimental data.

simulations of the notched bar using several α values from 0 to 1, and the appropriate value was the one best fitted to the experimental results [9].

The normalized experimental curves between strain fraction $\varepsilon/\varepsilon_f$ and time fraction t/t_f are shown in Figure 3. It can be seen that these curve shapes vary with different stress values. With the increase of the stress value, the contribution of tertiary creep strain toward the overall creep strain of the steel decreased. In addition, the plots between $\varepsilon/\varepsilon_f$ and t/t_f are the same for 70 and 82 MPa, and the same for 87 and 93 MPa. The shape of these curves depends on the fitted material constants λ, ρ, g and β according to eq. (10). Thus, three sets of material constants for a range of stresses can be obtained, which are listed in Table 1, marked as set 1, set 2 and set 3, respectively. Set 1 is fitted from 70 and 82 MPa (low stress region), set 2 is fitted from 87 and 93 MPa (middle stress region) and set 3 is fitted from 100 MPa (high stress region). Three creep damage tolerance factors λ can be obtained: high λ value is derived from low stresses, and relatively lower λ value is in order with the higher stress value. It has been demonstrated by Ashby and Dyson [6] that different creep damage tolerance factor λ will result in different characteristic shapes of creep curves, and correspondingly leading to different damage mechanisms. It has been concluded that λ value is between 1.5 and 2.5 when damage is caused by the growth of cavities in coupled diffusion and power-law creep, whereas, the value is above 4 when caused by microstructure degradation such as particles coarsening.

Table 1: Material constants sets obtained from low (70 and 82 MPa), middle (87 and 93 MPa) and high stress (100 MPa) regions at 650°C for P91 steel (stress in MPa and time in hours).

Stress sets	*B*	*n*	*A*	*υ*	*ρ*	*g*	*Φ*	*β*	*λ*
Set 1(low stresses)	1.092e-20	8.46	3.537e-17	7.35	0.2373	0.9841	3.959	1.706	6.683
Set 2 (middle stresses)	1.092e-20	8.46	3.537e-17	7.35	0.0432	0.9683	2.691	2.292	3.881
Set 3 (high stresses)	1.092e-20	8.46	3.537e-17	7.35	0.0163	0.7281	0.566	5.402	2.724

Comparisons of results calculated by different sets of material constants

Damage variables calculated using different sets of material constants

Creep continuum damage calculations are performed by ABAQUS, using these sets of material constants given in Table 1, respectively. The constants B, n, A and υ are the same in these sets, whereas varying λ and its corresponding derived ρ, g and Φ values will lead to different creep characteristics. Figure 4 shows the damage variable D/D_{cr} on the outer surface, as a function of time fraction t/t_f for material constant set 1 ($\lambda = 2.724$), set 2 ($\lambda = 3.881$) and set 3 ($\lambda = 6.683$) under the closed-end condition. These damage curves (Figure 4) have a similar variation with the normalized curves in Figure 3, which indicated the accuracy of modeling using these material constant sets. The damage condition becomes more serious as time increasing for all sets, and the contribution of the tertiary stage damage to the total damage decreases as the decreasing of λ value (set 1 > set 2 > set 3).

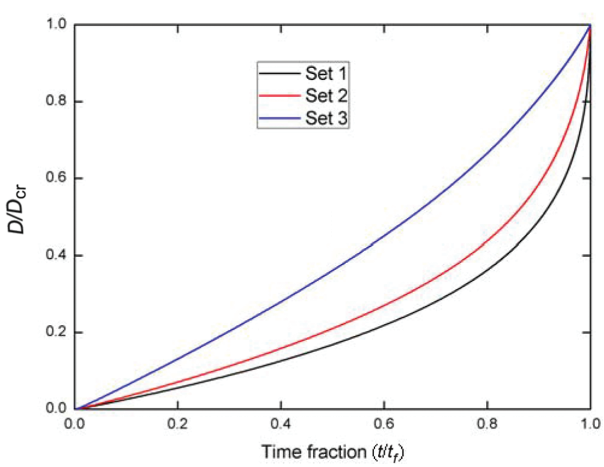

Figure 4: Damage variable D/D_{cr} as a function of time fraction (t/t_f) on the outer surface of the P91 pipe under the closed-end condition calculated by set 1 ($\lambda = 2.724$), set 2 ($\lambda = 3.881$) and set 3 ($\lambda = 6.683$).

Figures 5–7 show an example of damage variables through the pipe thickness at different times for sets 1–3, respectively. The analyzed times are t_f, $0.85t_f$, $0.65t_f$, $0.45t_f$ and $0.25t_f$, where t_f is the time when the damage

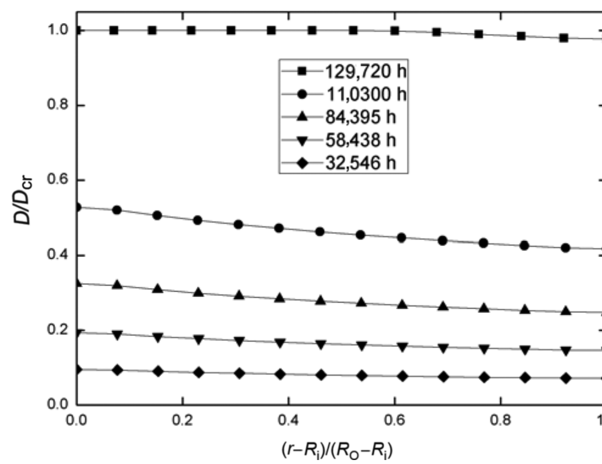

Figure 5: Damage history with the normalized distance along the pipe thickness starting from the outer surface, using set 1 shown in Table 1 ($t_f = 129{,}720$ h, $0.85t_f = 110{,}300$ h, $0.65t_f = 84{,}395$ h, $0.45t_f = 58{,}438$ h, $0.25t_f = 32{,}546$ h).

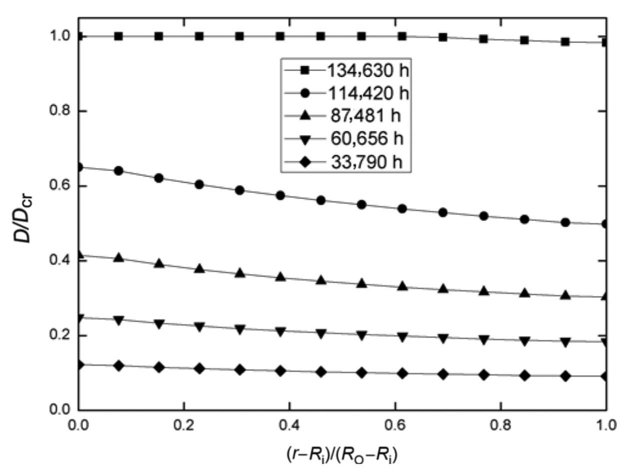

Figure 6: Damage history with the normalized distance along the pipe thickness starting from the outer surface, using set 2 shown in Table 1 ($t_f = 134{,}630$ h, $0.85t_f = 114{,}420$ h, $0.65t_f = 87{,}481$ h, $0.45t_f = 60{,}656$ h, $0.25t_f = 33{,}790$ h).

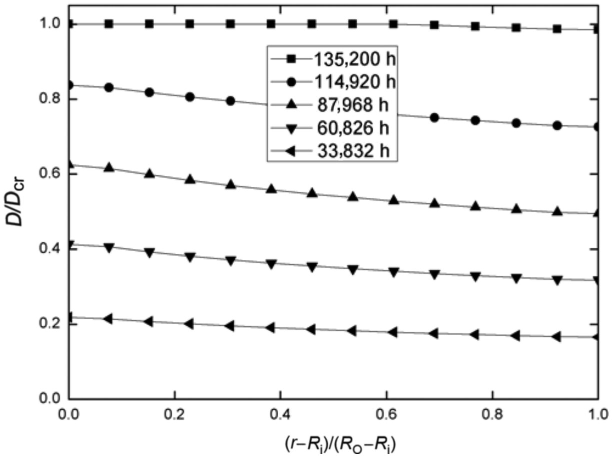

Figure 7: Damage history with the normalized distance along the pipe thickness starting from the outer surface, using set 3 shown in Table 1 ($t_f = 135{,}200$ h, $0.85t_f = 114{,}920$ h, $0.65t_f = 87{,}968$ h, $0.45t_f = 60{,}826$ h, $0.25t_f = 33{,}832$ h).

has extended to the whole pipe thickness for each set. The t_f values are 129,720 h for set 1, 134,630 h for set 2 and 135,200 h for set 3, indicating that the failure time increased with decreasing λ value (set 1 > set 2 > set 3). It can also be observed that the values of D/D_{cr} distributed much more uniform at different time intervals with the decreasing of λ value (set 1 > set 2 > set 3). However, the characteristic of the relationship between damage variation (D/D_{cr}) and pipe thickness is similar for different sets, i.e. the damage is decreasing from the inner to outer surface and the damage value is the highest approaching 1 at time t_f.

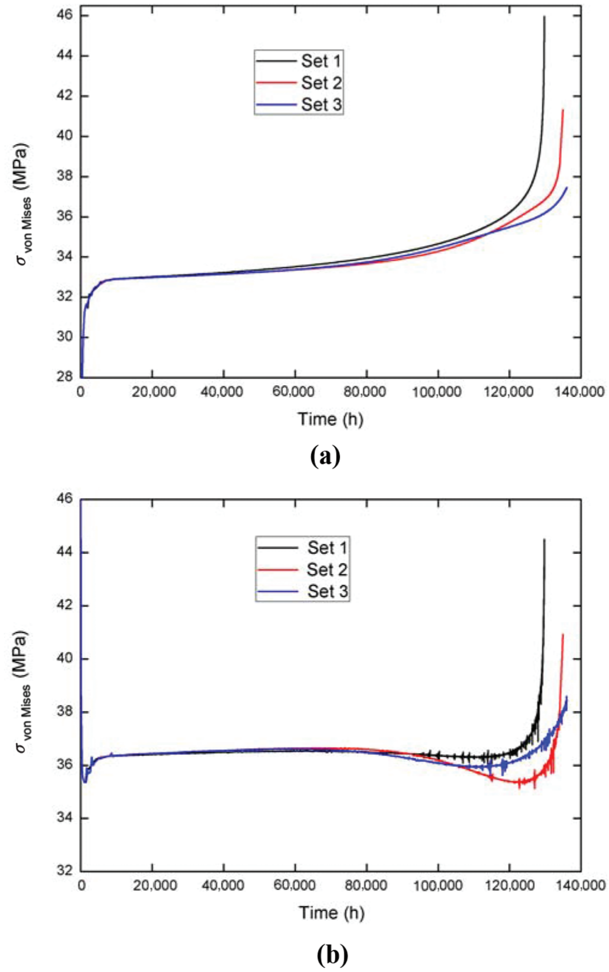

Figure 8: Variations of von Mises stress with time of the P91 pipe under closed-end condition calculated by set 1 ($\lambda = 2.724$), set 2 ($\lambda = 3.881$) and set 3 ($\lambda = 6.683$). (a) On the outer surface and (b) on the inner surface.

Stresses calculated using different sets of material constants

The variations of von Mises stresses on the outer and inner surfaces of the pipe, are calculated by different sets of material constants as shown in Figure 8(a) and 8(b), respectively. It can be seen that von Mises stresses are steady during the secondary stage on both surfaces. However, stresses on the outer surface are increasing rapidly during the primary and tertiary stages as time prolonging. On the other hand, stresses on the inner surface are decreasing during the primary and tertiary stages and then drastically increased at the rupture time point. From comparison of the results calculated by different material constants sets, it can also be observed that the primary and secondary stage are almost the same for all sets, whereas great difference has occurred during the tertiary stage, i.e. the ruptured von Mises stress for set 1 is the largest and value for set 2 is larger than set 3 correspondingly, from which it can be inferred that the decreasing λ value (set 1 > set 2 > set 3) can decrease the rupture stress value on both pipe surfaces.

The relationships between von Mises stress and pipe thickness at various creep times are shown in Figures 9, 10 and 11 for material set 1, set 2 and set 3, respectively. It is clear that stresses along the pipe thickness calculated by these sets all increased as time prolonging, and this increase is much more significant on the outer surface than on the inner surface. Great decreasing from set 1 to set 3 of the stress at the rupture time (t_f) can also been observed, that is about 44 MPa for set 1, 39.5 MPa for set 2 and 38 MPa for set 3. However, the stress distribution at the other times ($0.85t_f$, $0.65t_f$, $0.45t_f$ and

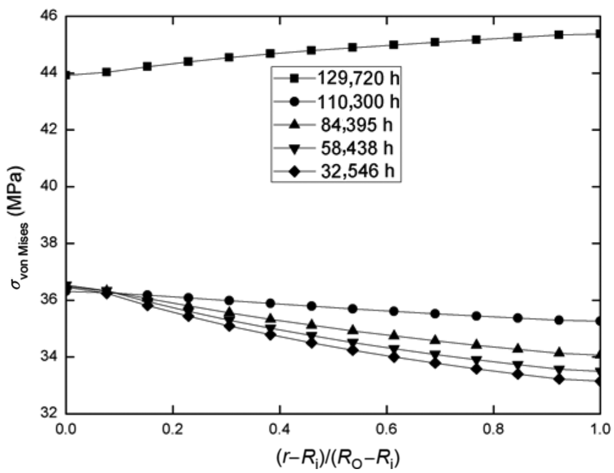

Figure 9: Von Mises stress variation history with the normalized distance along the pipe thickness starting from the outer surface, using set 1 shown in Table 1 ($t_f = 129{,}720$ h, $0.85t_f = 110{,}300$ h, $0.65t_f = 84{,}395$ h, $0.45t_f = 58{,}438$ h, $0.25t_f = 32{,}546$ h).

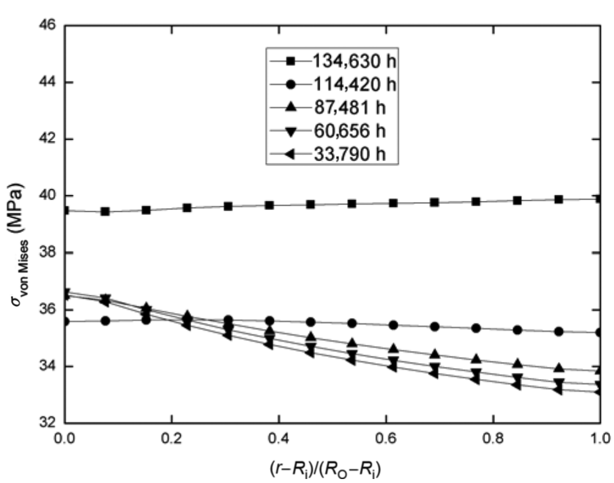

Figure 10: Von Mises stress variation history with the normalized distance along the pipe thickness starting from the outer surface, using material set 2 shown in Table 1 ($t_f = 134{,}630$ h, $0.85t_f = 114{,}420$ h, $0.65t_f = 87{,}481$ h, $0.45t_f = 60{,}656$ h, $0.25t_f = 33{,}790$ h).

$0.25t_f$) are similar for these sets, and the similarity is much more obvious especially at the lower times ($0.65t_f$, $0.45t_f$ and $0.25t_f$). This indicated that the decreasing λ value (set 1 > set 2 > set 3) has little influence during the primary and secondary stages, while can lead to a decreasing of stress as time prolonging to the rupture time during the tertiary stage.

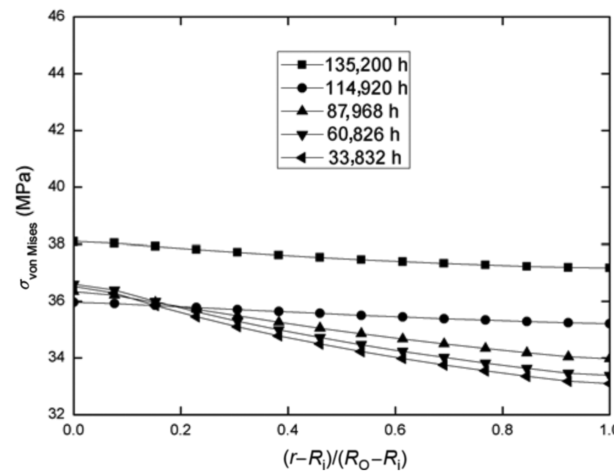

Figure 11: Von Mises stress variation history with the normalized distance along the pipe thickness starting from the outer surface, using material set 3 shown in Table 1 ($t_f = 135{,}200$ h, $0.85t_f = 114{,}920$ h, $0.65t_f = 87{,}968$ h, $0.45t_f = 60{,}826$ h, $0.25t_f = 33{,}832$ h).

Discussion

In consideration of time and economy saving, creep deformation and creep rupture data from high stresses performed by laboratory creep testing are used to simulate the characteristics of high temperature components serviced at lower stresses. However, the main difficulty with this method is that the material constants determined from high creep stress region may not be reliable for the simulation of creep behaviors within lower stress region. Thus, it is of significance to compare the results by using different material constants sets obtained from a relatively wide range of stresses.

In this paper, three sets of material constants are obtained for P91 steel at 650℃, where the creep tested stress ranges from 70 to 100 MPa. The obtained constants B, n, A and υ are the same in these sets. However, λ is decreasing from set 1 to set 3, which correspondingly leads to varying ρ, g and Φ values. The continuum damage models were used to evaluate the effect of these sets with decreasing λ on a closed-end condition pipe.

As the decreasing of λ value in different sets (set 1 > set 2 > set 3), the contribution of the tertiary stage to the total damage/strain becomes smaller, and the damage variable distribution at different time intervals becomes more uniform. This indicated that the model using material constants from higher stress region can obtain a more uniform damage among primary, secondary and tertiary stages.

Variation of von Mises stresses with time calculated by different sets showed similar characteristic. During the secondary stage, the stresses are all steady on both pipe surfaces. During the primary and tertiary stages, stresses on the outer surface are increasing while on the inner surface decreasing. Stresses along the pipe thickness all increased with time calculated by different sets, and this increasing is larger on the outer surface than on inner surface, which is in corresponding with the damage variation.

FE models using different material constants sets obtained from low, middle and high stress regions have slight difference on the primary and secondary stages. However, these sets have a great influence on the tertiary stage, that is when using decreasing λ value in different sets (set 1 > set 2 > set 3), the calculated rupture time and rupture stress will have a great difference. The material constants obtained from higher stress region can correspondingly cause higher rupture time and lower rupture stress. This is in close relationship with the damage contribution of the tertiary stage to total damage. The decreasing damage in tertiary stage calculated by decreasing λ value (higher stress region) can lead to higher rupture time and lower rupture stress; therefore, the simulation results of a structural component are much more conservative when using material constants determined from higher stress region. On the other hand, it is an unfortunate that the material constants sets are obtained from a relatively limited stress region (70–100 MPa), requiring further effort in later perfection of this method.

Conclusions

(1) Three sets of material constant sets were obtained from a range of stresses in creep testing for P91 steel at 650℃. In these sets, B, n, A and υ are the same, whereas λ value decreases from low to high stress region and correspondingly leads to varying ρ, g and Φ constants.

(2) The calculated damage versus time curve was compared with the experimental normalized strain versus time curve, and their variations are similar to each other. Thus, the accuracy of models conducted using different material constant sets could be verified.

(3) The results calculated by different material constant sets showed some similarity. During the secondary stage, stresses are all steady on both surfaces. During the primary and tertiary stages, stresses increase with time on the outer surface while decrease on the inner surface. Furthermore, both stress and damage along the pipe thickness increase with time when calculated by different sets, and this increasing is much larger on the outer surface than on the inner surface.

(4) The overall effect of different material constant sets lies on the tertiary stage of simulations, whereas little influence on the primary and secondary stages. That is, the rupture time increases and the corresponding rupture stress decreases, when calculated by material constants obtained from higher stress region (lower λ value). This is caused by the decreasing damage contribution of the tertiary stage to total damage when stress increasing. Thus, the simulation results of a structural component are much more conservative when using material constants determined from high stress region.

Acknowledgments: The authors would like to thank the High Temperature Technology Department and CAE Division for providing materials and heat treatment equipment.

Funding: This work was supported by the Postgraduate Cultivation and Innovation Project under the damage mechanism of 12Cr1MoV/P91 dissimilar joint after long-term creep program (grant no. KYLX_0750) and the Ningbo Natural Science Foundation under the technology of structure integrity assessment for dissimilar joints in utility boilers (grant no. 2009A610023).

References

[1] L.M. Kachanov, Theory of Creep edited by A.J. Kennedy, English Translation, National Lending Library, Boston Spa (1960).
[2] Y.N. Rabotnov, Creep Problems of Structural Members edited by F.A. Leckie, English Translation, Amsterdam, North Holland (1969).
[3] F.A. Leckie and D.R. Hayhurst, P. Roy. Soc. A., 340A (1974) 323–347.
[4] Y. Liu and S. Murakami, JSME Int. J., 41 (1998) 57–65.
[5] B.F. Dyson, J. Press. Vess-T. ASME, 122 (2000) 281–296.
[6] M.F. Ashby and B.F. Dyson, Volume 1 in Advances in Fracture Research edited by S.R. Valluri, Pergamon Press, Oxford (1984), pp. 3–30.
[7] Y. Liu, X.F. Sun and Q. Gao, Volume 3 in Proceedings of the VI International Conference on Material Mechanical Behaviour, ICM-6, July 29–August 2, 1991, Kyoto, Japan, Pergamon Press, Oxford (1991), pp. 859–864.
[8] T.H. Hyde, W. Sun and A.A. Becker, Int. J. Pres. Ves. Pip., 81 (2004) 363–371.
[9] T.H. Hyde, A.A. Becker, W. Sun and J.A. Williams, Int. J. Pres. Ves. Pip., 83 (2006) 853–863.